Journal of *Marine Science and Engineering*

MDPI

Article

Regional Assessment of the MFWAM Wave Model Around South America: Comparison with ERA5, WAVERYS, and Buoy Observations

Camila Parra-Urrea [1], Rodrigo Abarca-del-Rio [1,2,*], Lotfi Aouf [3] and Valeria Mundaca-Moraga [2]

[1] Doctoral Program in Energy, Faculty of Engineering, Universidad de Concepción, Concepción 4030000, Chile; camiparrau@udec.cl
[2] Department of Geophysics, Faculty of Physical and Mathematical Sciences, Universidad de Concepción, Concepción 4030000, Chile; valemundaca@udec.cl
[3] Centre National de Recherches Météorologiques (CNRM), Météo-France, 31057 Toulouse, France; lotfi.aouf@meteo.fr
* Correspondence: roabarca@udec.cl

Abstract

Accurate wave representation is essential for coastal engineering, navigation, and marine-energy applications. This study evaluates the original MFWAM wave-product outputs using a regional observational dataset assembled from 16 buoy stations across Chile, Colombia, Ecuador, and Brazil, with ERA5 and WAVERYS used as comparative reference products. Significant wave height (Hs), peak or mean wave period (Tp/Tm), and mean wave direction (Dm) were assessed over 2008–2025, depending on station availability, using statistical performance metrics, time series, scatter plots, and distributional analyses. High-wave conditions were additionally evaluated using the 95th and 99th percentiles of Hs. MFWAM showed its most consistent performance for Hs at the evaluated Chilean and southeastern Brazilian stations, with results generally comparable to ERA5 and WAVERYS. Wave-period performance was more variable among stations, while Dm exhibited stronger spatial variability and systematic discrepancies at some locations. For MFWAM, P95 and P99 differences relative to buoy observations generally remained within approximately ±15% at the stations where the product was available. Station-specific post-processing was applied as a secondary analysis at all evaluated stations and reduced persistent local discrepancies, although these results represent an in-sample assessment. Overall, the results identify both the strengths and limitations of MFWAM and establish an observation-based regional benchmark for its performance across the evaluated South American sectors, providing a basis for subsequent regional wave-climate and wave-energy assessments.

Keywords: MFWAM; ERA5; WAVERYS; wave model validation; buoy observations; significant wave height; wave period; mean wave direction; South America; CFOSAT

Check for updates

Academic Editor: Eugen Rusu

Received: 9 August 2026
Revised: 29 September 2026
Accepted: 30 September 2026
Published: 26 October 2026

Copyright: © 2026 by the authors. Licensee MDPI, Basel, Switzerland. This article is an open access article distributed under the terms and conditions of the Creative Commons Attribution (CC BY) license.

1. Introduction

Ocean waves constitute a fundamental component of ocean dynamics and air–sea interactions, influencing a wide range of processes, including maritime navigation, coastal engineering, and marine hazard assessment [1]. Accurate wave characterization is also essential for marine energy resource assessment, as the energy transported by waves depends primarily on significant wave height and wave period [2].

The assessment of wave climate at regional and global scales currently relies on in situ observations, satellite measurements, and numerical wave models. Among these,

reanalysis products and operational forecasting systems provide continuous time series and spatially homogeneous fields, making them valuable tools for climate studies, marine energy assessments, and coastal hazard analyses [3].

The validation of these products against in situ observations is a necessary step for evaluating their performance and determining their applicability across different oceanic regions. In South America, wave observations are mainly obtained from buoy networks operated by national institutions, providing an independent source of information for the assessment of numerical wave models and reanalysis products.

In recent years, satellite observations have significantly contributed to improving the representation of sea-state conditions. Among these, the CFOSAT (China–France Oceanography Satellite) mission, launched in 2018, was designed to provide global observations of surface winds and wave spectral characteristics. Since 2020, CFOSAT observations have been assimilated into the global MFWAM (Météo-France Wave Model) system as part of its operational data-assimilation framework [4].

Among the global wave products currently available, ERA5, developed by the European Centre for Medium-Range Weather Forecasts (ECMWF), WAVERYS, developed within the framework of the Copernicus Marine Environment Monitoring Service (CMEMS), and MFWAM, which incorporates the assimilation of CFOSAT observations, are widely used. ERA5 has been extensively employed for global and regional wave climate characterization owing to its long-term temporal coverage and global spatial consistency [3]. Likewise, wave reanalyses and numerical wave models have been widely applied to assess wave energy resources and wave climate variability in different regions of the world [2]. In South America, recent studies have used wave products to estimate wave energy potential and to analyze its spatial and temporal variability [5,6].

Within this context, the objective of the present study is to evaluate the performance of the original MFWAM wave-product outputs against ocean buoy observations across selected Pacific and Atlantic sectors of South America, using ERA5 and WAVERYS as comparative reference products. The analysis focuses on significant wave height (Hs), wave period (Tp or Tm, depending on station availability), and mean wave direction (Dm), considering statistical performance, the representation of observed distributions, and high-wave conditions through percentile-based metrics. Station-specific post-processing is additionally examined as a complementary in-sample analysis at the evaluated stations to quantify the potential reduction in persistent local discrepancies without replacing the validation of the original product outputs. This regional validation provides an observational basis for the future use of MFWAM in regional wave-climate studies and subsequent assessments of the spatial and seasonal variability of wave-energy resources around South America.

2. Materials and Methods

2.1. Observational Data

Wave observations from ocean buoys operated by the Chilean Hydrographic and Oceanographic Service (SHOA), the Brazilian National Buoy Program (PNBOIA), the Colombian Maritime Authority (DIMAR), and the Oceanographic and Antarctic Institute of the Ecuadorian Navy (INOCAR) were used in this study. These datasets have been widely employed in wave characterization and validation studies across South America [7–9].

The variables analyzed were significant wave height (Hs), wave period (Tp or Tm, depending on data availability at each station), and mean wave direction (Dm). Peak wave period (Tp) and mean wave period (Tm) represent distinct spectral properties and are therefore not treated as interchangeable variables. According to the observational datasets used in this study, Tp was available at Iquique, Antofagasta, Concón, Talcahuano, Bahía Solano, Barranquilla, Isla Gorgona, Jambelí, Manta, Salinas, Bacia de Santos, and Alcatrazes, whereas

Tm was available at Buenaventura, San Andrés–Providencia, Tumaco, and Turbo. Period-related comparisons were performed and interpreted according to the variable available at each station. Consequently, differences in period statistics between stations using Tp and those using Tm should not be interpreted solely as differences in wave climate or model performance. The observational records have an hourly temporal resolution and cover the period 2008–2025, depending on data availability at individual buoy stations.

Prior to comparison with the wave products, the observational data were subjected to quality-control procedures and temporal harmonization. The geographical location and measurement period of each buoy station are presented in Table 1.

Table 1. Geographic location and measurement period of the buoy stations initially considered in this study. Desertores and Punta Arenas were excluded from the final validation analysis.

Buoy Station	Latitude (°)	Longitude (°)	Start Date	End Date	Record Duration (Years)	Water Depth (m)
Iquique	−20.244	−70.246	4 June 2024	31 December 2025	1.6	18
Antofagasta	−23.735	−70.472	3 May 2024	28 December 2025	1.7	91
Concón	−32.862	−71.658	18 January 2024	31 December 2025	2	184
Talcahuano	−36.5667	−73.3389	15 June 2022	31 December 2025	3.6	125
Desertores	−42.771	−73.244	8 September 2022	31 December 2024	2.3	184
Punta Arenas	−53.097	−70.713	28 June 2023	31 December 2024	1.5	122
Bahía Solano	6.38	−77.722	3 September 2020	5 March 2024	3.5	-
Barranquilla	11.13	−74.81	11 April 2008	13 May 2019	11	-
Buenaventura	3.554	−77.722	2 December 2015	23 February 2020	4.2	-
Isla Gorgona	2.977	−78.252	13 October 2010	20 February 2019	8.4	-
San Andrés-Providencia	12.615	−81.682	12 March 2013	31 December 2020	7.8	-
Tumaco	1.917	−78.873	12 March 2008	24 July 2019	11.4	-
Turbo	8.911	−76.83	22 January 2010	7 October 2021	11.7	-
Alcatrazes	−24.1292	−45.6769	5 April 2022	30 August 2023	1.4	-
Bacia de Santos	−25.5182	−42.7352	10 December 2020	30 August 2023	2.7	-
Jambelí	−3.2102	−80.1485	29 August 2014	14 May 2015	0.7	20 m
Salinas	−2.1716	−80.9563	4 September 2013	25 November 2014	1.2	17 m
Manta	−0.9224	−80.7395	6 September 2013	30 April 2015	1.7	35 m

An initial set of 18 buoy stations was compiled from national ocean-monitoring networks in Chile [10], Colombia [11], Ecuador [12], and Brazil [13]. These stations include Iquique, Antofagasta, Concón, Talcahuano, Desertores, and Punta Arenas in Chile; Bahía Solano, Barranquilla, Buenaventura, Isla Gorgona, San Andrés, Tumaco, and Turbo in Colombia; Alcatrazes and Bacia de Santos in Brazil; and Jambelí, Salinas, and Manta in Ecuador.

Of the 18 initially compiled stations, the Desertores and Punta Arenas stations were excluded from the validation analysis due to their location within the fjord, channel, and archipelago region of southern Chile. Wave conditions at these sites are strongly influenced by local sheltering, complex coastal geometry, and bathymetric processes that are not fully resolved by the spatial resolution of the global wave products evaluated in this study. Consequently, the final validation dataset consisted of 16 buoy stations.

2.2. Numerical Wave Products

Three global wave products were used for validation against buoy observations. MFWAM (Météo-France Wave Model, Global Ocean Waves Analysis and Forecast) is a global wave model with a spatial resolution of 0.083° and a temporal resolution of 3 h. Since 2020, this product has incorporated observations from the CFOSAT (China–France Oceanography Satellite) mission through its data-assimilation system [4].

ERA5 (ECMWF Reanalysis v5) is the global atmospheric and oceanic reanalysis produced by the European Centre for Medium-Range Weather Forecasts (ECMWF), with a spatial resolution of 0.25° and an hourly temporal resolution [3].

WAVERYS is a global wave reanalysis developed within the framework of the Copernicus Marine Environment Monitoring Service (CMEMS), with a spatial resolution of 0.2°

and a temporal resolution of 3 h. The product is based on a previous version of MFWAM and incorporates the assimilation of satellite altimeter observations and directional wave spectra derived from Sentinel-1 measurements [6,14].

For each buoy station, the geographically nearest grid point from each wave product was selected based on the minimum absolute differences between the buoy and model-grid latitudes and longitudes. The corresponding model time series were extracted directly from the selected grid cell, without spatial interpolation. The geographical distance between the buoy and the selected grid point was calculated using the Haversine formula. Observation–model pairs were subsequently constructed for significant wave height (Hs), wave period (Tp/Tm), and mean wave direction (Dm).

2.3. Methodology

In this study, buoy observations were compared with the global wave products MFWAM, ERA5, and WAVERYS to evaluate their ability to represent wave conditions around South America. The analysis focused on significant wave height (Hs), wave period (Tp or Tm, depending on the variables available at each buoy station), and mean wave direction (Dm). For mean wave direction (Dm), error metrics and statistical indicators were interpreted considering the circular nature of directional data. For each station, model time series were extracted from the geographically nearest grid point without spatial interpolation, as described in Section 2.2. Observation–model pairs were then constructed through temporal matching. Subsequently, quality-control procedures were applied, statistical performance metrics were calculated, and complementary graphical analyses were conducted to assess the ability of the wave products to reproduce the temporal variability and statistical distribution of the observed wave conditions. All data processing, statistical analyses, and graphical representations were performed using MATLAB R2025b.

2.3.1. Temporal Matching and Quality Control

Buoy observations were standardized to a 3-h temporal resolution to ensure consistency with the analyzed wave products. For each station and wave product, common timestamps between observations and model outputs were identified, and observation–model pairs were constructed exclusively for coincident time records.

Records containing missing or invalid values in any of the analyzed variables (Hs, Tp/Tm, and Dm) were removed. In addition, a quality-control filter based on wave period was applied, excluding records that satisfied the condition defined in Equation (1):

$$|T_{mod} - T_{obs}| > 3\sigma_{T,mod} \quad (1)$$

where T_{mod} and T_{obs} denote the modeled and observed wave periods, respectively, and $\sigma_{T,mod}$ represents the standard deviation of the modeled wave period. Wave period, particularly peak wave period, is sensitive to differences in spectral frequency discretization between numerical wave models and buoy measurements. Bedossa et al. [15], in their validation of MFWAM against drifting-buoy observations, similarly applied quality-control criteria to collocated wave data, including the exclusion of records exhibiting large model–observation differences in peak period. Following the same general rationale, the present criterion uses a station- and product-dependent threshold based on three times the standard deviation of the modeled wave period, allowing the threshold to scale with the variability of the local modeled wave conditions. The resulting temporal mask was applied consistently to the analyzed wave parameters to maintain temporally matched observation–model datasets. This procedure was implemented as an a priori quality-control step before calculating the validation statistics.

The effect of the quality-control procedure on data availability was quantified for each station and wave product using the number of observation–model pairs available before and after filtering, together with the corresponding percentage of excluded records. The resulting sample sizes are reported in Table S7 of the Supplementary Materials.

2.3.2. Station-Specific Post-Processing Procedures

The primary validation was conducted using the original, unadjusted outputs of MFWAM, ERA5, and WAVERYS in order to assess the intrinsic performance of each wave product against buoy observations. Station-specific corrections were subsequently applied as a secondary post-processing analysis to quantify the potential reduction in persistent local biases. This distinction allows the validation of the original wave products to remain independent of the observation-based corrections, while the corrected results are interpreted exclusively as an in-sample assessment of the potential value of local post-processing.

Hs and Tp/Tm

For Hs and Tp/Tm, the corrected model values were obtained using the linear relationship defined in Equation (2):

$$M_{corr} = aM + b \quad (2)$$

where M represents the original modeled time series, M_{corr} the bias-corrected time series, and a and b are the slope and intercept of the linear adjustment, respectively. The coefficients were estimated separately for each station, wave product, and wave-period or wave-height variable using ordinary least squares regression of the buoy observations against the corresponding modeled values. The slope a is dimensionless and represents a multiplicative scaling factor, whereas the intercept b represents an additive offset with the same units as the corrected variable. These coefficients are specific to the observational period and location used for their estimation and should not be interpreted as universal correction factors or as recommended values for other stations.

This procedure was used to quantify the extent to which station-specific scaling and offset adjustments could reduce systematic differences between modeled and observed values within the analyzed period. The corrected results are interpreted as an assessment of the potential value of local post-processing and do not replace the validation of the original product outputs. Accordingly, the unadjusted results are used to characterize baseline product performance, whereas the corrected results are used to evaluate the additional reduction in persistent local scaling and offset differences.

Because the correction coefficients were estimated using the same observation–model pairs included in the corrected assessment, these results represent an in-sample post-processing evaluation rather than an independent validation of the correction. Consequently, the corrected metrics quantify the achievable local improvement within the analyzed periods but should not be interpreted as evidence of identical performance during independent periods or at unmonitored locations.

Mean wave direction (Dm)

For mean wave direction (Dm), the baseline validation was performed using the original modeled directions. For each observation–model pair, the angular difference was calculated and wrapped within the interval from -180° to 180°. Circular Bias, angular MAE, and angular RMSE were calculated from these original differences, without previously removing the mean angular offset. The angular correction was subsequently applied as a second stage to quantify the additional improvement achievable through local post-processing.

Due to the circular nature of the mean wave direction (Dm), linear angular differences may produce artificially large biases when directions are close to the $0^\circ/360^\circ$ bound-

ary. Therefore, the bias correction applied to Dm was based on a constant angular offset computed from the mean circular angular bias between the observations and the model simulations. The angular difference was calculated using Equation (3):

$$err_i = atan2[sin(D_{obs,i} - D_{mod,i}), cos(D_{obs,i} - D_{mod,i})] \quad (3)$$

The mean circular angular bias was then computed using Equation (4):

$$\delta = atan2(sin(err), cos(err)) \quad (4)$$

Finally, the corrected modeled direction was obtained by applying a constant angular offset, as shown in Equation (5):

$$D_{corr} = mod(D_{mod} + \delta, 360^\circ) \quad (5)$$

where D_{obs} and D_{mod} denote the observed and modeled wave directions, respectively; δ is the mean circular angular bias, and D_{corr} is the corrected modeled direction. This procedure removes the systematic directional bias while preserving the temporal variability of the simulated time series.

The primary validation and conclusions are based on the original, unadjusted wave-product outputs. Selected corrected results are presented in the main manuscript as illustrative examples of the station-specific post-processing, while the complete corrected results are provided in the Supplementary Materials as a secondary in-sample assessment. The complete set of station- and product-specific adjustment coefficients for Hs and Tp/Tm, together with the circular directional offsets for Dm, is provided in Table S10 of the Supplementary Materials.

2.3.3. Statistical Performance Assessment

Model performance was evaluated using mean bias (Bias), root mean square error (RMSE), mean absolute error (MAE), the Pearson correlation coefficient (R), the coefficient of determination (R^2), and the scatter index (SI). These metrics are widely used in the validation of wave models and wave products [16,17].

For Hs and Tp/Tm, the statistical metrics were computed using the conventional formulations of Bias, RMSE, MAE, the Pearson correlation coefficient (R), the coefficient of determination (R^2), and the scatter index (SI). For the mean wave direction (Dm), Bias, RMSE, and MAE were computed using circular angular differences to avoid discontinuities associated with the $0^\circ/360^\circ$ boundary.

Mean bias was calculated using Equation (6):

$$Bias = \frac{1}{N}\sum_{i=1}^{N}(M_i - O_i) \quad (6)$$

where (M_i) and (O_i) represent the modeled and observed values, respectively, and (N) denotes the number of observation–model pairs.

The mean absolute error was calculated using Equation (7):

$$MAE = \frac{1}{N}\sum_{i=1}^{N}|M_i - O_i| \quad (7)$$

The root mean square error was calculated using Equation (8):

$$RMSE = \sqrt{\frac{1}{N}\sum_{i=1}^{N}(M_i - O_i)^2} \quad (8)$$

The Pearson correlation coefficient was calculated using Equation (9):

$$R = \frac{\sum_{i=1}^{N}(M_i - \overline{M})(O_i - \overline{O})}{\sqrt{\sum_{i=1}^{N}(M_i - \overline{M})^2}\sqrt{\sum_{i=1}^{N}(O_i - \overline{O})^2}} \quad (9)$$

The coefficient of determination was defined using Equation (10):

$$R^2 \quad (10)$$

Finally, the scatter index (*SI*) was calculated using Equation (11):

$$SI = \frac{RMSE}{\overline{O}} \times 100 \quad (11)$$

where $\overline{O}$ represents the mean observed value.

Beyond the primary validation metrics, complementary statistics were calculated to characterize the dispersion and distributional properties of the observed and modeled data. These include standard deviation, mean absolute deviation (MAD), centered RMSE (CRMSE), their normalized counterparts, skewness, and kurtosis. These metrics are intended to provide additional information on the ability of the wave products to reproduce the observed variability and distributional characteristics. The complete complementary statistics are reported in Tables S4–S6 of the Supplementary Materials for Hs, Tp/Tm, and Dm, respectively.

2.3.4. Descriptive Statistics

To complement the error-based performance assessment, descriptive statistics were calculated for both observed and modeled distributions, including the minimum, first quartile (Q1), median, third quartile (Q3), and maximum values. These statistics were used to characterize the distributions of Hs, Tp, Tm, and Dm and to support the interpretation of the boxplots.

In addition, the upper tail of the Hs distribution was assessed using the 95th percentile (P95) for both buoy observations and the corresponding wave products. The difference ΔP95 = P95_product − P95_buoy was used to quantify the overestimation or underestimation of high-wave conditions. The 99th percentile (P99) was also calculated as a secondary indicator of the upper tail of the Hs distribution.

2.3.5. Comparative Graphical Analysis

The comparison between observations and model simulations was complemented through the use of time series, scatter plots, and boxplots. Time series were used to evaluate the temporal evolution of the analyzed variables, whereas scatter plots were employed to examine the relationship between observations and simulations relative to the one-to-one line. Boxplots were used to characterize the central tendency, dispersion, distributional range, and outliers of each variable [6].

3. Results

This section presents the validation results following a progressive structure. First, the stations used to evaluate the wave products are described. A detailed analysis of the Talcahuano station, located in south-central Chile and selected as a representative case study, is then presented. For this station, the time series of each variable, their comparison with the MFWAM, ERA5, and WAVERYS products, the scatter plots, boxplots, and statistical performance metrics are examined. The results for the complete set of stations are subsequently presented and discussed, beginning with an overall assessment

of product performance for each variable, followed by a country-level analysis and, finally, an evaluation of their ability to represent the observed high-wave conditions.

3.1. Overview of the Validation Stations

Following the station-selection procedure described in Section 2.1, a total of 16 ocean buoy stations distributed across selected Pacific and Atlantic coastal sectors of Chile, Colombia, Ecuador, and Brazil were retained for the final validation analysis in this study (Figure 1). These stations provide a broad range of oceanographic and climatic conditions for wave-model evaluation. Table 1 summarizes the main characteristics of each station, including its name, geographical location, and period of data availability. The in situ records span the period 2008–2025; however, due to differences in observational network availability, the length of the records varies among stations. Consequently, comparisons between regions should be interpreted in the context of the effective observation period available at each buoy. The observational records differ substantially in duration, ranging from less than one year at Jambelí to more than 11 years at Barranquilla, Tumaco, and Turbo (Table 1). Several stations, including Iquique, Antofagasta, Concón, Alcatrazes, Jambelí, Salinas, and Manta, have records shorter than two years, whereas Isla Gorgona, San Andrés–Providencia, Barranquilla, Tumaco, and Turbo provide substantially longer observational periods. Therefore, results from stations with shorter records should be interpreted as representative of model performance during the available sampling period rather than as long-term climatological characterizations.

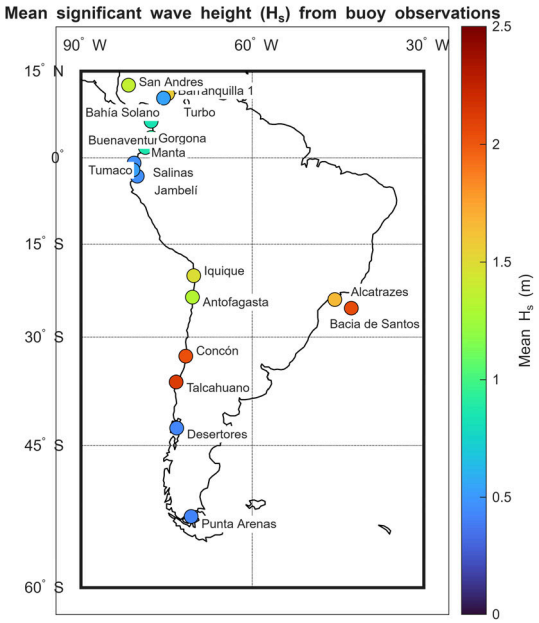


Figure 1. Location of the 18 buoy stations initially considered in the study. Desertores and Punta Arenas were excluded from the final validation analysis. Colors indicate the mean significant wave height (Hs) at the stations retained for validation.

The datasets were obtained from regional oceanographic and meteorological institutions, including SHOA (Chile), PNBOIA (Brazil), DIMAR (Colombia), and INOCAR (Ecuador). These observations constitute the reference dataset used for the validation of the wave products and the statistical analyses presented in the following sections.

3.2. Validation at the Representative Talcahuano Station

Talcahuano was selected as a representative station to illustrate the main characteristics of the comparison between buoy observations and the original, unadjusted ERA5,

WAVERYS, and MFWAM outputs. Time series, scatter plots, and distributional comparisons are shown in Figures 2–4. The scatter plots in Figure 3 report the main validation metrics directly in each panel, while the boxplots in Figure 4 summarize the distributional characteristics of the observed and modeled variables.

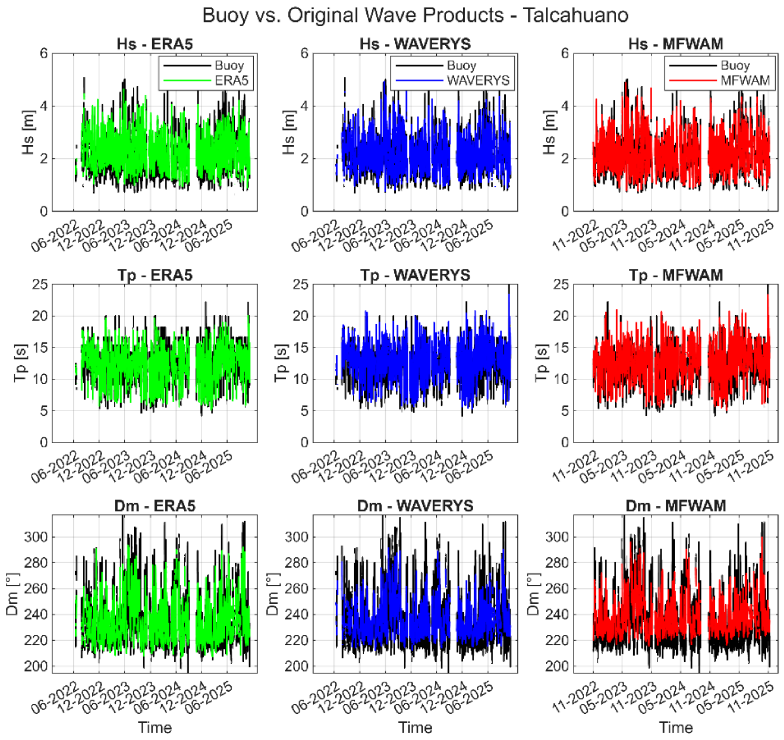


Figure 2. Comparative time series of buoy observations and the original, unadjusted ERA5, WAVERYS, and MFWAM outputs for Hs, Tp, and Dm at the Talcahuano station.

For significant wave height (Hs), the three products reproduce the temporal variability observed at the buoy, although differences are evident in both dispersion and error magnitude. WAVERYS and MFWAM show stronger agreement with the observations than ERA5, with correlation coefficients of 0.939 and 0.938 and RMSE values of 0.238 and 0.244 m, respectively, compared with R = 0.888 and RMSE = 0.337 m for ERA5 (Figure 3). All three products show a positive bias, which is larger for ERA5 (0.126 m) than for WAVERYS (0.040 m) and MFWAM (0.067 m). The boxplots further show that the observed median Hs is closely reproduced, although the products underestimate the highest observed Hs values and exhibit a somewhat narrower upper range than the buoy observations (Figure 4).

For peak wave period (Tp), differences among the products are smaller. Correlations range from 0.750 to 0.776 and RMSE values from 1.73 to 1.77 s, indicating comparable point-by-point agreement among ERA5, WAVERYS, and MFWAM (Figure 3). The boxplots indicate that median values are also close to the observed value, although the modeled distributions do not reproduce the full observed range. The buoy record extends from 4.20 to 25.00 s, whereas the modeled values span a narrower interval. The scatter plots further show increasing dispersion at longer observed periods (Figures 3 and 4).

The points displayed beyond the boxplot whiskers represent values outside 1.5 times the interquartile range. These values were retained in the analysis after application of the a priori quality-control procedure described in Section 2.3.1 and were not subjected to an additional post hoc outlier-removal step.

For mean wave direction (Dm), all products reproduce the dominant directional range, but exhibit a positive directional bias relative to the buoy observations. ERA5 presents the lowest RMSE (9.71°) and the smallest bias (1.56°), followed by WAVERYS (RMSE = 10.80°,

Bias = 2.51°) and MFWAM (RMSE = 11.30°, Bias = 4.72°), while correlations remain similar among the three products (R = 0.829–0.850) (Figure 3). The boxplots show that the observed median direction is reasonably reproduced, although all products present a narrower directional range than the buoy observations (Figure 4).

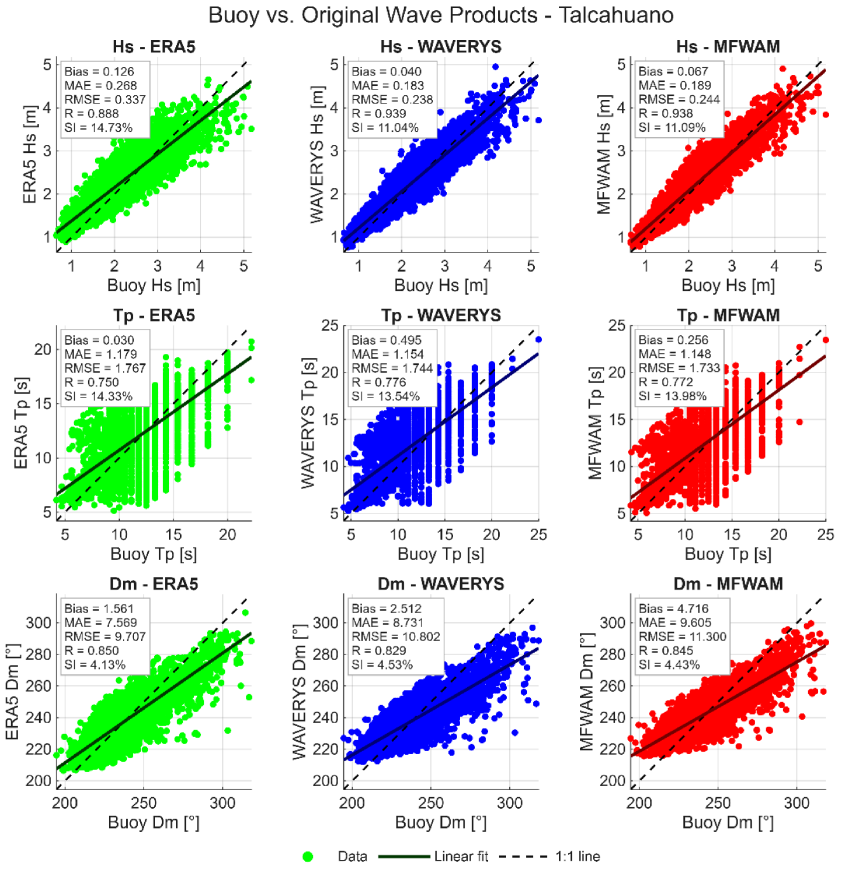


Figure 3. Scatter plots comparing buoy observations with the original, unadjusted ERA5, WAVERYS, and MFWAM outputs for Hs, Tp, and Dm at the Talcahuano station. Colored dots represent matched observation–model pairs, solid colored lines represent the linear fit to the data, and black dashed lines indicate the 1:1 line. Bias, MAE, RMSE, R, and SI are reported in each panel.

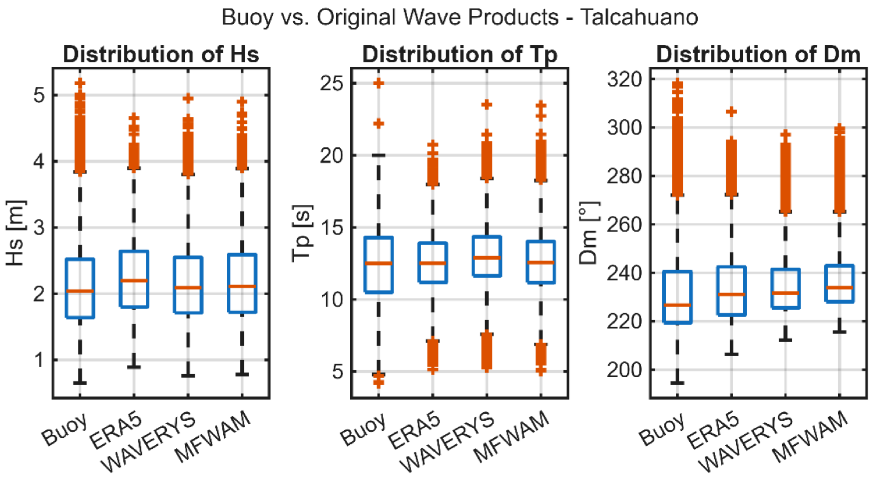


Figure 4. Comparison of observed and modeled distributions of Hs, Tp, and Dm at the Talcahuano station using the original, unadjusted ERA5, WAVERYS, and MFWAM outputs. Boxes represent the interquartile range (Q1–Q3), central lines indicate the median, and whiskers extend to the most extreme values within 1.5 times the interquartile range. Points beyond the whiskers are statistical outliers according to the boxplot convention.

Overall, the Talcahuano comparison shows stronger agreement for Hs in WAVERYS and MFWAM, broadly comparable performance among the three products for Tp, and similar directional skill for Dm. The corresponding station-specific corrected results are provided in the Supplementary Materials and are interpreted as a secondary in-sample post-processing assessment.

3.3. Results for All Stations

The regional assessment focuses primarily on the performance of MFWAM against buoy observations around South America, using ERA5 and WAVERYS as reference products to contextualize its performance under the same comparison framework. The results discussed in the main manuscript correspond to the original, unadjusted wave-product outputs. Complete station-level validation statistics, including both unadjusted and station-specific adjusted results, are provided in Tables S1–S3 of the Supplementary Materials. Complementary dispersion and distributional metrics are reported in Tables S4–S6. To avoid repetitive station-by-station descriptions, the main patterns are summarized below by wave variable and geographical region, while detailed distributional statistics are reported in Figures S1–S3 and Table S8. At the Ecuadorian stations, where MFWAM results were not available, ERA5 and WAVERYS are retained to provide regional context but are not used to assess MFWAM directly.

3.3.1. Significant Wave Height (Hs)

For significant wave height (Hs), MFWAM shows consistent performance at the Chilean stations, with correlations ranging from 0.869 to 0.938 and RMSE values between 0.217 and 0.318 m for the original unadjusted outputs. The strongest agreement is observed at Iquique, Concón, and Talcahuano, where MFWAM performs at a level comparable to WAVERYS and, in several cases, with lower errors than ERA5. At Talcahuano, for example, MFWAM reaches R = 0.938 and RMSE = 0.244 m, while at Iquique it presents an RMSE of 0.217 m and an almost negligible bias of 0.009 m.

In southeastern Brazil, MFWAM also reproduces Hs variability well. At Bacia de Santos and Alcatrazes, correlations reach 0.922 and 0.948, respectively, with RMSE values of 0.269 and 0.266 m. These values are of the same order as those obtained with ERA5 and WAVERYS, indicating that MFWAM maintains a performance comparable to the reference products under the wave conditions represented at these stations.

In Colombia, MFWAM is available at Bahía Solano, where it yields R = 0.826 and RMSE = 0.182 m. These values are comparable in magnitude to those obtained with ERA5 and WAVERYS, although the correlation is somewhat lower. The remaining Colombian stations show a wider range of performance in the reference products, from high correlations at San Andrés to very weak agreement at Turbo, illustrating the greater spatial heterogeneity of model performance in this region.

To provide a visual comparison of MFWAM performance across these regional settings, Figure 5 presents buoy-observation versus original, unadjusted MFWAM Hs scatter plots for Concón (Chile), Bahía Solano (Colombia), and Bacia de Santos (Brazil).

At the Ecuadorian stations, only ERA5 and WAVERYS are available. These results therefore provide regional context rather than a direct assessment of MFWAM. WAVERYS exhibits substantially smaller biases and RMSE values than ERA5 at Jambelí, Manta, and Salinas, while ERA5 shows positive Hs biases of approximately 0.56–0.73 m.

Overall, the Hs results indicate that MFWAM consistently reproduces the observed wave-height variability at the stations where it is available, particularly in Chile and Brazil, with performance generally comparable to the two reference products. This provides a strong observational basis for subsequent applications that depend on an accurate representation of significant wave height.

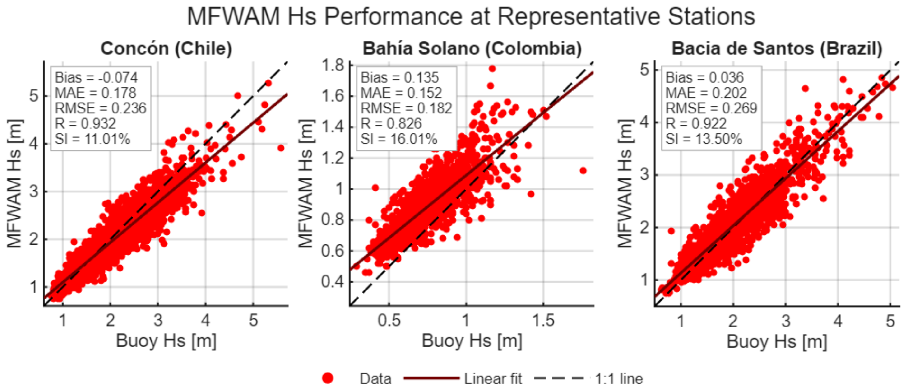


Figure 5. Scatter plots comparing buoy observations with the original, unadjusted MFWAM significant wave height (Hs) outputs at three representative stations: Concón (Chile), Bahía Solano (Colombia), and Bacia de Santos (Brazil). Colored dots represent matched observation–model pairs, solid lines represent the linear fit to the data, and black dashed lines indicate the 1:1 line. Bias, MAE, RMSE, R, and SI are reported in each panel.

3.3.2. Wave Period (Tp/Tm)

For wave period, MFWAM shows relatively homogeneous performance across the Chilean stations. For Tp, correlations range from 0.729 to 0.772 and RMSE values from 1.69 to 1.85 s in the original outputs. These results are generally comparable to those obtained with ERA5 and WAVERYS, and no single product consistently exhibits the lowest error at all stations. At Talcahuano, MFWAM reaches R = 0.772 and RMSE = 1.733 s, while at Concón it reaches R = 0.761 and RMSE = 1.761 s.

In Brazil, MFWAM maintains correlations close to 0.70–0.74, although errors are somewhat larger than at the Chilean stations. At Bacia de Santos, it presents RMSE = 2.233 s and R = 0.698, whereas at Alcatrazes it reaches RMSE = 1.833 s and R = 0.744. ERA5 and WAVERYS show values of the same general order, although they produce lower RMSE values at some locations.

At Bahía Solano, MFWAM shows larger discrepancies for Tp, with RMSE = 3.484 s and R = 0.604. The reference products also show greater errors at this station than at several Chilean locations, indicating stronger regional dependence in the representation of wave period. Elsewhere in Colombia, both Tp and Tm are reported depending on the buoy, and these variables should be interpreted separately because they represent different spectral properties of the wave field.

At the Ecuadorian stations, where MFWAM is not available, the comparison between the reference products shows that WAVERYS has lower RMSE values and higher correlations at Jambelí and Manta, whereas ERA5 performs more favorably at Salinas. These results are included to characterize the regional behavior of the reference products and should not be interpreted as an evaluation of MFWAM in Ecuador.

Overall, the results indicate that MFWAM provides a reasonably consistent representation of wave period in Chile and Brazil, with performance generally comparable to ERA5 and WAVERYS, while larger discrepancies occur at Bahía Solano. The regional variability observed for this parameter should therefore be considered in applications that depend on modeled wave-period information.

3.3.3. Mean Wave Direction (Dm)

For mean wave direction (Dm), MFWAM exhibits greater spatial variability in performance than for Hs. In Chile, the strongest agreement is observed at Concón and Talcahuano. At Concón, MFWAM reaches R = 0.902 and RMSE = 7.984° for the original outputs, while

at Talcahuano it reaches R = 0.845 and RMSE = 11.300°. In both cases, its performance is comparable to that obtained with ERA5 and WAVERYS.

In contrast, Iquique exhibits a pronounced systematic directional offset. MFWAM presents a circular bias of 79.35° and an RMSE of 80.47°, despite maintaining a moderate correlation of R = 0.582. A similar behavior is observed for ERA5 and WAVERYS, whose directional biases also exceed 80°. This indicates that the discrepancy is not specific to MFWAM and also demonstrates that correlation alone does not fully describe systematic directional offsets.

In Brazil, MFWAM maintains a high correlation at Bacia de Santos (R = 0.914) and a moderate correlation at Alcatrazes (R = 0.730), with RMSE values of 24.63° and 24.44°, respectively. At Bahía Solano in Colombia, MFWAM reaches R = 0.801 and RMSE = 20.13°, within the same general order as ERA5 and WAVERYS. Overall, these results show that MFWAM reproduces directional variability reasonably well at several stations, but systematic directional offsets remain important at specific locations.

At the Ecuadorian stations, only ERA5 and WAVERYS are available. Both products show substantial negative directional biases at Jambelí, Manta, and Salinas, with particularly large RMSE values at Manta. These results demonstrate that large directional offsets also occur in the reference products in this region, but they do not provide a direct assessment of MFWAM performance in Ecuador.

The station-specific circular correction substantially reduces directional offsets at several locations. However, because these corrections were derived using the same observations employed for evaluation, the corrected results are interpreted only as a secondary in-sample post-processing assessment and are therefore reported in the Supplementary Materials rather than used to characterize the baseline performance of MFWAM.

Overall, the regional validation shows that MFWAM consistently reproduces significant wave height at the stations where it is available, with performance generally comparable to ERA5 and WAVERYS, particularly in Chile and southeastern Brazil. Wave-period performance is also broadly comparable to the reference products, although larger regional differences are evident at some locations. Mean wave direction shows the greatest spatial variability and the largest systematic discrepancies, emphasizing the need to consider local directional biases when interpreting model output. Taken together, these results identify both the strengths and limitations of MFWAM in representing wave conditions around South America and provide the observational basis for its subsequent use in regional wave-climate applications.

3.3.4. Representation of High-Wave Conditions

The representation of high-wave conditions was assessed using the 95th percentile (P95) of Hs rather than individual maximum values, which are more sensitive to isolated events and record length. The 99th percentile (P99) was additionally examined as a secondary indicator of the upper tail of the Hs distribution.

MFWAM generally reproduced the upper Hs distribution with moderate differences relative to buoy observations. The smallest P95 differences were found at Talcahuano (−0.03 m; −0.9%) and Bacia de Santos (−0.03 m; −0.8%), followed by Iquique (−0.10 m; −4.1%) and Concón (−0.19 m; −6.1%). Larger differences were observed at Antofagasta (+0.23 m; +11.0%), Bahía Solano (+0.15 m; +13.5%), and Alcatrazes (−0.37 m; −13.5%). For P99, the relative differences for MFWAM ranged from approximately −12.9% at Alcatrazes to +14.5% at Bahía Solano.

ERA5 and WAVERYS exhibited stronger regional variability in the representation of the upper Hs distribution. The largest P95 overestimations occurred at the Ecuadorian stations, particularly for ERA5, while underestimation was observed at several Colom-

bian stations. Overall, the percentile-based assessment shows that the representation of high-wave conditions varies geographically among the evaluated wave products and complements the conventional error and correlation metrics by directly examining the upper tail of the Hs distribution.

3.3.5. Station-Specific Post-Processing

As a secondary analysis, the effect of the station-specific post-processing was examined at Talcahuano. The correction reduced the systematic biases of Hs, Tp, and Dm to values close to zero for ERA5, WAVERYS, and MFWAM. For Hs, the RMSE decreased from 0.337 to 0.312 m for ERA5, from 0.238 to 0.233 m for WAVERYS, and from 0.244 to 0.235 m for MFWAM. For Tp, the corresponding RMSE decreased from 1.767 to 1.699 s, from 1.744 to 1.621 s, and from 1.733 to 1.656 s, respectively. The reduction was also observed for Dm, with RMSE decreasing from 9.707° to 9.587° for ERA5, from 10.802° to 10.522° for WAVERYS, and from 11.300° to 10.299° for MFWAM.

To further illustrate the effect of the station-specific post-processing on MFWAM Hs across different regional settings, Table 2 compares the original and linearly adjusted results at the same three representative stations shown in Figure 5. At Concón, the adjustment reduces RMSE from 0.236 to 0.223 m and MAE from 0.178 to 0.169 m. A larger reduction is observed at Bahía Solano, where RMSE decreases from 0.182 to 0.117 m and MAE from 0.152 to 0.090 m. In contrast, at Bacia de Santos, the changes are small, with RMSE remaining at 0.269 m and MAE decreasing only slightly from 0.202 to 0.201 m. These results illustrate that the effect of the station-specific adjustment varies among stations and should therefore be interpreted as an in-sample post-processing assessment rather than as independent evidence of improved predictive skill.

Table 2. MFWAM significant wave height (Hs) validation statistics at the three representative stations shown in Figure 5, comparing the original, unadjusted outputs with the station-specific linearly adjusted results. The adjusted values represent an in-sample post-processing assessment.

Station	Adjustment	Bias (m)	MAE (m)	RMSE (m)	R	SI (%)
Concón	Unadjusted	−0.074	0.178	0.236	0.932	11.014
Concón	Linear adjustment	0.000	0.169	0.223	0.932	10.960
Bahía Solano	Unadjusted	0.135	0.152	0.182	0.826	16.010
Bahía Solano	Linear adjustment	0.000	0.090	0.117	0.826	15.440
Bacia de Santos	Unadjusted	0.036	0.202	0.269	0.922	13.504
Bacia de Santos	Linear adjustment	0.000	0.201	0.269	0.922	13.639

These results illustrate the extent to which station-specific post-processing can reduce persistent local discrepancies within the analyzed dataset. Because the correction coefficients were derived and evaluated using the same observations, these results represent an in-sample assessment and are not interpreted as an independent improvement in predictive skill. The complete corrected results for all stations are provided in the Supplementary Materials.

4. Discussion

The validation based on the original wave-product outputs shows that MFWAM reproduces significant wave height (Hs) consistently at most stations where it is available. In Chile, MFWAM Hs RMSE values range from 0.217 to 0.318 m, with correlation coefficients between 0.869 and 0.938. Similar agreement is found in southeastern Brazil, where RMSE values are 0.269 m at Bacia de Santos and 0.266 m at Alcatrazes, with R = 0.922 and 0.948, respectively. At Bahía Solano, the only Colombian station where MFWAM was available, RMSE = 0.182 m and R = 0.826. Overall, MFWAM performance for Hs is generally

comparable to ERA5 and WAVERYS, although the relative differences among products remain station-dependent.

Wave-period performance is more variable than that observed for Hs. At the Chilean stations, MFWAM Tp RMSE values are approximately 1.7–1.9 s, with correlations generally between 0.73 and 0.77, showing performance of the same overall order as ERA5 and WAVERYS. Larger discrepancies occur at some stations outside Chile, including Bahía Solano and Bacia de Santos. These comparisons should also consider that some stations provide peak wave period (Tp), whereas others provide mean wave period (Tm). Because these variables describe different spectral properties of the sea state, comparisons among stations should be interpreted accordingly.

Mean wave direction (Dm) shows greater spatial variability and stronger systematic discrepancies than Hs. Performance depends markedly on station and product, particularly at locations affected by complex coastal geometry or strongly directional wave regimes. These differences may reflect bathymetric effects, wave refraction, coastal sheltering, locally generated waves, and limitations associated with the spatial resolution of global products. The circular nature of Dm also requires particular attention, since conventional linear differences may lead to misleading interpretations when directions are close to the 0°/360° boundary.

The percentile-based analysis provides additional information on the representation of high-wave conditions. For MFWAM, P95 differences relative to buoy observations range from approximately −13.5% at Alcatrazes to +13.5% at Bahía Solano, while differences are below 1% at Talcahuano and Bacia de Santos. P99 shows a similar overall behavior, with relative differences remaining within approximately ±15% at the stations where MFWAM is available. ERA5 and WAVERYS also exhibit substantial regional variability, including marked P95 overestimation at some Ecuadorian stations and underestimation at several Colombian stations. Thus, satisfactory performance according to conventional error and correlation metrics does not necessarily imply an equally accurate representation of the upper portion of the Hs distribution.

Wave conditions along the Brazilian coast have previously been characterized mainly through reanalysis products and numerical modeling. Ref. [18] assessed the wave energy resource along the coast of Santa Catarina using ERA-Interim and reported mean values of Hs = 1.76 m and T = 8.07 s. At a broader spatial scale, ref. [19] reported significant wave heights of approximately 1.5–2.0 m and characteristic periods of 8–9 s along the southern and southeastern Brazilian coast. More locally, ref. [20] investigated the wave climate around the Alcatrazes Archipelago and reported typical Hs values between 1.0 and 2.0 m, peak periods of 7–10 s, and dominant wave directions from the east, southeast, and south. In the present study, buoy observations at Bacia de Santos show median values of Hs = 1.86 m, Tp = 9.1 s, and Dm = 119°, whereas at Alcatrazes the corresponding medians are Hs = 1.29 m, Tp = 9.3 s, and Dm = 137°. These values are consistent with the characteristic ranges reported in previous studies [18–20], while the present validation additionally quantifies how ERA5, WAVERYS, and MFWAM reproduce the observed conditions.

Previous studies in Colombia have also relied largely on numerical simulations and reanalysis products. Ref. [21] reported an average significant wave height of approximately 1.01 m and a mean wave period of about 6.14 s for energetic Colombian regions, while ref. [22] identified typical Hs values between 0.5 and 2.0 m in the northern Caribbean and predominant waves from the east to east-northeast. In the present observations, median Hs values are 1.51 m at Barranquilla, 1.36 m at San Andrés–Providencia, and 0.44 m at Turbo. Median wave periods are approximately 7.0 s at Barranquilla and 5.0 s at San Andrés and Turbo. The values at Barranquilla and San Andrés are broadly consistent with the ranges reported by [21,22], whereas Turbo reflects substantially lower-energy local conditions. The

inclusion of long-term buoy observations from both the Caribbean and Pacific coasts therefore complements the predominantly model-based assessments available for Colombia.

For Ecuador, ref. [23] reported significant wave heights of approximately 1.5–2.0 m and characteristic periods of 12–15 s, while ref. [24] used buoy observations from Salinas to validate a high-resolution WAVEWATCH III hindcast. In the present study, median Hs values are lower, reaching 0.31 m at Jambelí, 0.44 m at Manta, and 0.50 m at Salinas, whereas median wave periods of approximately 14.3 s at Jambelí and Manta and 15.4 s at Salinas are consistent with the period range previously reported. These differences emphasize the importance of direct observational characterization and may partly reflect differences in location, observation period, and the wave statistics considered. The present analysis additionally provides a direct evaluation of ERA5 and WAVERYS against observations at the three Ecuadorian stations.

In Chile, previous studies have described energetic swell-dominated conditions and a latitudinal increase in wave activity toward central and southern regions. Ref. [25] reported frequent Hs values of 2.5–3.5 m and energetic periods of approximately 9–11 s in central Chile, whereas the Chilean Wave Atlas developed by [26] provided a long-term climatological description of wave conditions along the coast. Wave-energy assessments based on numerical simulations and instrumental measurements have also identified persistently energetic conditions along central-southern Chile [8]. From a longer-term perspective, ref. [27] reported characteristic Hs values around 1.5 m and peak periods of 10–11 s during earlier decades, while more recent studies have evaluated ERA5 performance [28] and updated the Chilean Wave Atlas using WAVEWATCH III [29]. In the present observations, median Hs increases from 1.46 m at Iquique and 1.27 m at Antofagasta to 1.97 m at Concón and 2.04 m at Talcahuano, with peak periods close to 12.5 s at several stations. This spatial pattern is consistent with the stronger wave conditions previously described toward central and central-southern Chile [25–27]. Unlike the climatological approaches used in many previous studies, the present work directly evaluates multiple global wave products against station-based observations.

The station-specific post-processing provides complementary information but does not alter the interpretation of the baseline validation. At Talcahuano, the adjustment reduces persistent local biases and decreases RMSE for several variables and products. However, because the correction coefficients were derived and evaluated using the same observation–model pairs, these results constitute an in-sample assessment rather than independent evidence of improved predictive skill. Consequently, the conclusions regarding MFWAM performance are based on the original outputs, whereas the corrected results illustrate the potential reduction in local systematic discrepancies when observations are available.

The station-specific coefficients reported in Table S10 show substantial variability among stations and wave products, indicating that the magnitude and sign of the required adjustments are strongly location-dependent. Therefore, the present results do not support defining universal recommended coefficient ranges for ERA5, WAVERYS, or MFWAM; establishing transferable ranges would require independent calibration and validation across additional stations and observational periods.

Taken together, this validation provides an observational basis for future regional applications requiring reliable information on wave height, period, and direction. The spatially continuous fields provided by MFWAM can support subsequent analyses of regional and seasonal wave variability around South America, including future applications related to marine and wave-energy resource characterization. ERA5 and WAVERYS remain valuable complementary datasets for inter-product comparison and uncertainty assessment.

Study Limitations and Perspectives

The main limitations of this study are related to the spatial and temporal availability of in situ observations. The buoy stations cover different periods and are unevenly distributed around South America; consequently, regional comparisons should not be interpreted as direct climatological comparisons between identical periods. A denser observational network would allow the validation to be extended to a larger number of regions and would provide a more detailed characterization of the conditions under which each wave product performs well or poorly.

MFWAM was also unavailable at several stations, particularly in Colombia and Ecuador, limiting simultaneous three-product comparisons across the complete observational network. In addition, the use of the nearest model grid point may introduce representativeness differences at coastal stations, where local bathymetry, wave refraction, sheltering, locally generated waves, and other nearshore processes may not be fully resolved by global wave products.

Previous studies have investigated wave conditions and wave-energy resources in countries such as Argentina [30–32], Uruguay [33–35], and Peru [36–39]. However, the buoy datasets used in these regions were not available for inclusion in the present study. Despite efforts to contact the responsible institutions, including the Servicio de Hidrografía Naval (SHN) in Argentina, the Servicio de Oceanografía, Hidrografía y Meteorología de la Armada (SOHMA) in Uruguay, and the Dirección de Hidrografía y Navegación (DHN) in Peru, access to suitable observational records could not be obtained. In contrast, Colombia (DIMAR) and Ecuador (INOCAR) provided access to their buoy records, while observational datasets from Brazil (PNBOIA) and Chile (SHOA) are publicly available. The regional coverage of the present validation should therefore be interpreted in light of these observational constraints.

The P95 and P99 analysis provides a robust description of the upper portion of the Hs distribution but does not constitute a formal extreme-value analysis or provide long-return-period estimates. Such analyses would require sufficiently long and temporally consistent observational records. Future studies based on longer records could complement the percentile-based assessment with extreme-value methods and return-period estimates.

An additional limitation concerns the ability of global wave products to represent smaller-scale coastal processes. Although nearest-grid-point comparison provides a consistent framework for regional validation, it does not necessarily reproduce all processes that may modify wave conditions locally in areas of complex bathymetry and coastal geometry. In addition to refraction, sheltering, and other bathymetric effects, recent studies have shown that interactions between waves and periodic seabed topography can produce Bragg reflection and influence resonance processes in coastal and harbor environments [40–43]. These mechanisms operate at spatial scales that are not explicitly resolved by the global products considered here and are therefore outside the scope of the present regional validation. Nevertheless, they should be considered in future studies involving high-resolution coastal downscaling, particularly in areas characterized by complex geometry, periodic bathymetric features, or potential local resonance.

Future work should therefore extend the present validation using additional in situ observations, independent periods for evaluating station-specific post-processing, and higher-resolution coastal modeling capable of resolving local processes that are not represented by global products. The integration of MFWAM with coastal downscaling approaches could provide a more detailed assessment of bathymetric effects, refraction, Bragg reflection, and local resonance, while also extending the applicability of the validated information to regional and coastal wave-climate studies and future wave-energy resource assessments.

5. Conclusions

This study evaluated MFWAM against buoy observations from selected Pacific and Atlantic sectors of Chile, Colombia, Ecuador, and Brazil, using ERA5 and WAVERYS as comparative reference products. The validation based on the original outputs shows that MFWAM provides consistent performance for significant wave height, particularly at the evaluated Chilean and southeastern Brazilian stations, with results generally comparable to those of the reference products. Wave-period performance is more variable among stations, while mean wave direction exhibits stronger spatial variability and systematic discrepancies at some locations.

The percentile-based assessment further shows that the representation of high-wave conditions depends on both location and product. At the stations where MFWAM is available, P95 and P99 differences are generally moderate, although both underestimation and overestimation occur. These results highlight the importance of complementing conventional validation statistics with distribution-based metrics when assessing the upper portion of the Hs distribution.

The comparison with previous studies shows that the buoy observations analyzed here are broadly consistent with previously reported regional wave conditions in Chile, Brazil, Colombia, and Ecuador [18–29], while extending those studies through a common observational validation of multiple global wave products. Station-specific post-processing can reduce persistent local discrepancies, as illustrated at Talcahuano, but because the corrections were assessed in-sample, they are interpreted only as a secondary analysis and not as independent evidence of improved predictive performance.

Overall, the results identify both the strengths and limitations of MFWAM and establish an observation-based regional benchmark for its performance across the South American sectors for which suitable buoy records could be assembled. This benchmark provides a basis for subsequent analyses of regional and seasonal wave variability and future wave-energy resource assessments. ERA5 and WAVERYS remain valuable complementary references for inter-product comparison and uncertainty assessment. At coastal scales, future studies should complement these global products with higher-resolution modeling and consider local processes associated with coastal geometry and bathymetry, including refraction, reflection, and resonance mechanisms that are not explicitly resolved in the present evaluation.

Supplementary Materials: The following supporting information can be downloaded at: https://www.mdpi.com/article/10.3390/jmse14212006/s1, Tables S1–S3, validation statistics; Tables S4–S6, complementary statistical metrics; Table S7, Tp/Tm filtering summary; Figures S1–S3 and Table S8, distributional summaries; Table S9, high-wave percentile assessment; and Table S10, station-specific adjustment coefficients.

Author Contributions: Conceptualization, R.A.-d.-R., C.P.-U. and V.M.-M.; methodology, C.P.-U., R.A.-d.-R. and L.A.; software, C.P.-U. and V.M.-M.; validation, C.P.-U.; formal analysis, C.P.-U. and R.A.-d.-R.; investigation, C.P.-U. and R.A.-d.-R.; data curation, C.P.-U.; writing—original draft preparation, C.P.-U.; writing—review and editing, R.A.-d.-R. and L.A.; visualization, C.P.-U. and R.A.-d.-R.; supervision, R.A.-d.-R. and L.A. All authors have read and agreed to the published version of the manuscript.

Funding: C.P.-U. acknowledges funding from the Agencia Nacional de Investigación y Desarrollo (ANID), Programa de Formación de Capital Humano Avanzado (PFCHA), Doctorado Nacional 2023, grant ANID-PFCHA/Doctorado Nacional/2023-21232317.

Institutional Review Board Statement: Not applicable.

Informed Consent Statement: Not applicable.

Data Availability Statement: ERA5 data are available through the Copernicus Climate Data Store, while WAVERYS and MFWAM data are available through the Copernicus Marine Service. Buoy observations were obtained from the data providers identified in the manuscript. Processed data may be made available by the corresponding author upon reasonable request, subject to the policies of the original data providers.

Acknowledgments: The authors express their sincere appreciation to the reviewers for their thorough and constructive feedback during the major revision process. Their insightful comments prompted substantial additional analysis and significantly enhanced the scientific rigor and clarity of this manuscript. We are especially grateful to A. L. (DIMAR, Colombia) and S. M. (INOCAR, Ecuador) for their kind assistance in providing access to the observational buoy datasets used in this study. Furthermore, we thank SHOA (Chile) and PNBOIA (Brazil) for making their buoy observations publicly available. Finally, we acknowledge Météo-France, ECMWF, and the Copernicus Marine Service for the wave products utilized in this study. C.P.-U. gratefully acknowledges the support of the Institut français du Chili and the Dirección de Relaciones Internacionales (DRI) of the Universidad de Concepción for the fellowship that made a research stay at Météo-France possible, enabling the completion of this manuscript. The authors also thank the Météo-France team for providing a welcoming environment, as well as for their scientific insights and valuable contributions to the completion of this study.

Conflicts of Interest: The authors declare no conflicts of interest.

Abbreviations

The following abbreviations are used in this manuscript:

MFWAM	Météo-France Wave Model
CFOSAT	China–France Oceanography Satellite
ERA5	ECMWF Reanalysis v5
ECMWF	European Centre for Medium-Range Weather Forecasts
WAVERYS	Copernicus global wave reanalysis
CMEMS	Copernicus Marine Environment Monitoring Service
Hs	significant wave height
Tp	peak wave period
Tm	mean wave period
Dm	mean wave direction
RMSE	root mean square error
MAE	mean absolute error
SI	scatter index
SHOA	Chilean Hydrographic and Oceanographic Service
PNBOIA	Brazilian National Buoy Program
DIMAR	Colombian Maritime Authority
INOCAR	Oceanographic and Antarctic Institute of the Ecuadorian Navy

References

1. Holthuijsen, L.H. *Waves in Oceanic and Coastal Waters*; Cambridge University Press: Cambridge, UK, 2007.
2. Gunn, K.; Stock-Williams, C. Quantifying the Global Wave Power Resource. *Renew. Energy* **2012**, *44*, 296–304. [CrossRef]
3. Hersbach, H.; Bell, B.; Berrisford, P.; Hirahara, S.; Horányi, A.; Muñoz-Sabater, J.; Nicolas, J.; Peubey, C.; Radu, R.; Schepers, D.; et al. The ERA5 Global Reanalysis. *Q. J. R. Meteorol. Soc.* **2020**, *146*, 1999–2049. [CrossRef]
4. Aouf, L.; Hauser, D.; Chapron, B.; Toffoli, A.; Tourain, C.; Peureux, C. New Directional Wave Satellite Observations: Towards Improved Wave Forecasts and Climate Description in Southern Ocean. *Geophys. Res. Lett.* **2021**, *48*, e2020GL091187. [CrossRef]
5. Mundaca-Moraga, V.; Abarca-del-Rio, R.; Figueroa, D.; Morales, J. A Preliminary Study of Wave Energy Resource Using an HF Marine Radar, Application to an Eastern Southern Pacific Location: Advantages and Opportunities. *Remote Sens.* **2021**, *13*, 203. [CrossRef]
6. Mundaca-Moraga, V.; Abarca-del-Rio, R. Wave Energy Potential and the Role of Extreme Events on South America's Coasts. A Regional Frequency Analysis. *Appl. Ocean Res.* **2024**, *153*, 104280. Correction in *Appl. Ocean Res.* **2025**, *154*, 104338. [CrossRef]
7. Dragani, W.C.; Martin, P.B.; Simionato, C.G.; Campos, M.I. Are Wind Wave Heights Increasing in South-Eastern South American Continental Shelf between 32° S and 40° S? *Cont. Shelf Res.* **2010**, *30*, 481–490. [CrossRef]

8. Lucero, F.; Catalán, P.A.; Ossandón, Á.; Beyá, J.; Puelma, A.; Zamorano, L. Wave Energy Assessment in the Central-South Coast of Chile. *Renew. Energy* **2017**, *114*, 120–131. [CrossRef]
9. Shadman, M.; Roldan-Carvajal, M.; Pierart, F.G.; Haim, P.A.; Alonso, R. A Review of Offshore Renewable Energy in South America: Current Status and Future Perspectives. *Sustainability* **2023**, *15*, 1740. [CrossRef]
10. Servicio Hidrográfico y Oceanográfico de la Armada de Chile. *Serie de Datos de Oleaje Del Centro Nacional de Datos Hidrográficos y Oceanográficos de Chile (CENDHOC) [Subconjuntos Utilizados: Iquique (2024-06-04–2025-12-31); Antofagasta (2024-05-03–2025-12-28); Concón (2024-01-18–2025-12-31); Talcahuano (2022-06-15–2025-12-31); Desertores (2022-09-08–2024-12-31); Punta Arenas (2023-06-28–2024-12-31)]*; Servicio Hidrográfico y Oceanográfico de la Armada de Chile (SHOA): Valparaíso, Chile, 2026.
11. Dirección General Marítima. *Serie de Datos de Oleaje Obtenidos Por La Red de Medición de Parámetros Oceanográficos y de Meteorología Marina (RedMpomm) [Subconjuntos Utilizados: Bahía Solano (2020-09-03–2024-03-05); Barranquilla (2008-04-11–2019-05-13); Buenaventura (2015-12-02–2020-02-23); Isla Gorgona (2010-10-13–2019-02-20); San Andrés–Providencia (2013-03-12–2020-12-31); Tumaco (2008-03-12–2019-07-24); Turbo (2010-01-22–2021-10-07)]*; Dirección General Marítima (DIMAR), Centro de Investigaciones Oceanográficas e Hidrográficas (CIOH): Bogotá, Colombia, 2024.
12. Instituto Oceanográfico y Antártico de la Armada. *Serie de Datos de Oleaje de Boyas Oceanográficas [Subconjuntos Utilizados: Jambelí (2014-08-29–2015-05-14); Salinas (2013-09-04–2014-11-25); Manta (2013-09-06–2015-04-30)]*; Instituto Oceanográfico y Antártico de la Armada (INOCAR): Guayaquil, Ecuador, 2015.
13. Centro de Hidrografia da Marinha. *Dados Meteoceanográficos Do Programa Nacional de Boias (PNBOIA) [Subconjuntos Utilizados: Alcatrazes (2022-04-05–2023-08-30); Bacia de Santos (2020-12-10–2023-08-30)]*; Centro de Hidrografia da Marinha (CHM): Niterói, Brazil, 2023.
14. Law-Chune, S.; Aouf, L.; Dalphinet, A. WAVERYS: A CMEMS Global Wave Reanalysis during the Altimetry Period. *Ocean Dyn.* **2021**, *71*, 357–378. [CrossRef]
15. Bedossa, E.; Aouf, L.; Hauser, D.; Dalphinet, A.; Giordani, H.; Collard, F. Long Term Assimilation of Directional Wave Data From CFOSAT in the Wave Prediction Model MFWAM. *Earth Space Sci.* **2026**, *13*, e2025EA004743. [CrossRef]
16. Willmott, C.; Matsuura, K. Advantages of the Mean Absolute Error (MAE) over the Root Mean Square Error (RMSE) in Assessing Average Model Performance. *Clim. Res.* **2005**, *30*, 79–82. [CrossRef]
17. Wilks, D.S. *Statistical Methods in the Atmospheric Sciences*, 3rd ed.; Academic Press: Oxford, UK, 2011.
18. Contestabile, P.; Ferrante, V.; Vicinanza, D. Wave Energy Resource along the Coast of Santa Catarina (Brazil). *Energies* **2015**, *8*, 14219–14243. [CrossRef]
19. Espindola, R.L.; Araújo, A.M. Wave Energy Resource of Brazil: An Analysis from 35 Years of ERA-Interim Reanalysis Data. *PLoS ONE* **2017**, *12*, e0183501. [CrossRef]
20. Takase, L.S.; Stein, L.P.; Hoff, N.T.; Siegle, E. Wave Climate and Power Distribution around a Rocky Island: Alcatrazes, Brazil. *Ocean Coast. Res.* **2021**, *69*, e21010. [CrossRef]
21. Osorio, A.F.; Ortega, S.; Arango-Aramburo, S. Assessment of the Marine Power Potential in Colombia. *Renew. Sustain. Energy Rev.* **2016**, *53*, 966–977. [CrossRef]
22. Solano Rincones, J.D. Evaluación Del Potencial Energético Undimotriz En El Norte de La Costa Caribe Colombiana. Master's Thesis, Universidad del Norte, Barranquilla, Colombia, 2022.
23. Chimbo Campuzano, M.J.; Rodriguez Santos, R.R. Aprovechamiento de la Energía Undimotriz en el Ecuador. *Ingenius* **2016**, *17*, 23–28. [CrossRef]
24. Corrales-Gonzalez, M.; Lavidas, G.; Lira-Loarca, A.; Besio, G. Wave Energy Assessment and Wave Converter Applicability at the Pacific Coast of Central America. *Front. Energy Res.* **2024**, *12*, 1454275. [CrossRef]
25. Mediavilla, D.; Sepúlveda, H. Energía Undimotriz En Chile Continental: Zonas de Generación Del Oleaje y Predictibilidad. Ph.D. Thesis, Universidad de Concepción, Concepción, Chile, 2016.
26. Beyá, J.; Álvarez, M.; Gallardo, A.; Hidalgo, H.; Winckler, P. Generation and Validation of the Chilean Wave Atlas Database. *Ocean Model.* **2017**, *116*, 16–32. [CrossRef]
27. Ulazia, A.; Penalba, M.; Rabanal, A.; Ibarra-Berastegi, G.; Ringwood, J.; Sáenz, J. Historical Evolution of the Wave Resource and Energy Production off the Chilean Coast over the 20th Century. *Energies* **2018**, *11*, 2289. [CrossRef]
28. Selman-Caro, D.; Gorr-Pozzi, E.; Odériz, I.; Díaz-Hernández, G.; García-Nava, H.; Silva, R. Assessing Wave Energy for Possible WEC Installations at La Serena, Central Chile. *Ocean Eng.* **2024**, *295*, 116854. [CrossRef]
29. Correa Araya, S.O.; Aguirre, C.; Becerra, D.; Molina, M.; Vilchez, P.; Bahamóndez, S. Upgrade of the Chilean Wave Atlas Database. *Ocean Model.* **2025**, *193*, 102456. [CrossRef]
30. Echevarría, E.R.; Dragani, W.C.; Wörner, S. A Comprehensive Study about Alongshore Wave Energy Flux in the Coast of Buenos Aires, Argentina. *J. Coast. Conserv.* **2019**, *23*, 435–443. [CrossRef]
31. Salimbeni, A.; Dragani, W.; Alonso, G. Ocean Waves in the Southwestern Atlantic Ocean: An Evaluation of Global Wave Models. *Int. J. Climatol.* **2024**, *44*, 2725–2738. [CrossRef]

32. Battaglia, L.; Storti, M.A.; Rojas, L.; Dotti, F.E. Caracterización Del Oleaje En El Estuario de Bahía Blanca Para La Obtención de Energía Undimotriz. *Mecánica Comput.* **2025**, *41*, 1255–1264. [CrossRef]
33. Alonso Hauser, R. Evaluación Del Potencial Undimotriz de Uruguay. Master's Thesis, Universidad de La República (Uruguay), Montevideo, Uruguay, 2012.
34. Alonso, R.; Solari, S. Comprehensive Wave Climate Analysis of the Uruguayan Coast. *Ocean Dyn.* **2021**, *71*, 823–850. [CrossRef]
35. Alonso, R.; Solari, S.; Teixeira, L. Wave Energy Resource Assessment in Uruguay. *Energy* **2015**, *93*, 683–696. [CrossRef]
36. López, M.; Veigas, M.; Iglesias, G. On the Wave Energy Resource of Peru. *Energy Convers. Manag.* **2015**, *90*, 34–40. [CrossRef]
37. Villanueva Soto, P.O. Diseño de Un Sistema de Generación Undimotriz Tipo Captador Puntual Para Generar Electricidad En La Zona Norte Del Perú. Bachelor's Thesis, Universidad Católica Santo Toribio de Mogrovejo, Chiclayo, Peru, 2022.
38. Avellaneda Vasquez, L.S.; Perez Hernandez, P.A. Evaluación Del Potencial Undimotriz En La Costa de Pimentel Para Generar Energía Eléctrica. Bachelor's Thesis, Universidad César Vallejo, Chiclayo, Peru, 2024.
39. De La Torre, D.; Ortega, A. Variability and Wave Power for Open Ocean Wave Conditions of the Peru Basin. In Proceedings of the 2022 IEEE Engineering International Research Conference (EIRCON), Lima, Peru, 26–28 October 2022; IEEE: Piscataway, NJ, USA, 2022; pp. 1–4. [CrossRef]
40. Hou, L.; Gao, J. Investigations on alleviation effect of Bragg breakwater on harbor resonance induced by irregular waves. *Ocean Eng.* **2026**, *353*, 124797. [CrossRef]
41. Gao, J.; Hou, L.; Liu, Y.; Shi, H. Influences of Bragg reflection on harbor resonance triggered by irregular wave groups. *Ocean Eng.* **2024**, *305*, 117941. [CrossRef]
42. Gao, J.; Shi, H.; Zang, J.; Liu, Y. Mechanism analysis on the mitigation of harbor resonance by periodic undulating topography. *Ocean Eng.* **2023**, *281*, 114923. [CrossRef]
43. Gao, J.; Ma, X.; Dong, G.; Chen, H.; Liu, Q.; Zang, J. Investigation on the effects of Bragg reflection on harbor oscillations. *Coast. Eng.* **2021**, *170*, 103977. [CrossRef]

Disclaimer/Publisher's Note: The statements, opinions and data contained in all publications are solely those of the individual author(s) and contributor(s) and not of MDPI and/or the editor(s). MDPI and/or the editor(s) disclaim responsibility for any injury to people or property resulting from any ideas, methods, instructions or products referred to in the content.